Journal of The
Electrochemical Society

Outstanding Platinum Recovery by Electrochemical Cathodic Leaching and Redeposition in One-Pot 2 M HCL Solution

To cite this article: Mariappan Sakthivel *et al* 2025 *J. Electrochem. Soc.* **172** 074509

Journal of The Electrochemical Society, 2025 **172** 074509

Outstanding Platinum Recovery by Electrochemical Cathodic Leaching and Redeposition in One-Pot 2 M HCL Solution

Mariappan Sakthivel, Reshma Gandharva, Christopher Schreiber, and Jean-Francois Drillet[*,z]

Energy Storage and Conversion, DECHEMA-Forschungsinstitut, 60486 Frankfurt am Main, Germany

Selective Pt recovery from spent Pt/C gas diffusion electrodes (GDE) is essential for sustainable proton exchange membrane fuel cell and electrolysis industry. This study presents a promising, environmentally friendly approach using pulsed electrochemical cathodic leaching (ECCL) and subsequent electrochemical cathodic deposition (ECCD) in one pot diluted HCl solution. The parameters of ECCL pulse signal were optimized by varying electrolyte concentration, cell voltage, duty cycle, pulse number, and pulse sequence. For aging of GDE, a standard accelerated degradation tests protocol was applied. The amount of dissolved Pt in the electrolyte was evaluated by UV–vis absorption peak intensity at 260 nm that is assigned to Pt (IV) chloro complex ions. A Pt dissolution rate of 99.8% from fresh and aged GDE was achieved in 2 M HCl by applying cell voltage of "only" −3 V (cathode potential: −0.55 V vs RHE) and combining long and short pulse voltage sequences. Remaining Pt in the electrode were determined from electrochemical surface area and thermogravimetric analysis profiles confirming UV–vis results. Finally, proof of concept of one-pot Pt recovery from ECCL electrolyte by means of ECCD step was demonstrated.
 [DOI: 10.1149/1945-7111/adecc6]

Manuscript submitted February 12, 2025; revised manuscript received June 6, 2025. Published July 16, 2025.

Supplementary material for this article is available online

On the way to net-zero CO_2 emission target by 2050, emerging hydrogen fuel cell technology and more especially low-temperature PEM fuel cell, might bring significant decarbonization benefits for automotive and heavy transport applications.[1] However, both polymer electrolyte membrane fuel cell (PEMFC) and polymer electrolyte membrane electrolysis (PEMEL) technologies rely on expensive platinum as catalyst whose yearly global production amounts only to about 220 tons, from which 100 tons are used as exhaust catalysts.[2] Moreover, Platinum group of metals (PGM) are listed as critical raw materials (CRMs) by EU commission.[3] The present cost of a PEMFC stack in high volume production line is about $ 75 per kW of which 40% of cost is attributed to catalyst layer alone.[4] Beyond the cost of platinum, the natural resources of Pt ore are limited to principally South Africa and Russia mines in which about 85% of total Pt pure metal is produced. To reduce the costs and accelerate market penetration, the U.S. Department of Energy (DOE) set Pt catalyst loading for automotive application to maximum 0.125 mg cm^{-2} as target.[5] For a 100 kW fuel cell car, about 15–25 g Pt are usually needed that is not far from DOE target of 0.125 mg cm^{-2} by 2020.[6] For PEM electrolyzer on industrial scale, state-of-the art of Pt loading amounts about 0.5–1.0 mg cm^{-2}. By assuming a cell voltage of approximately 2 V, this equates to about 0.25–0.5 mg_{Pt} W^{-1} (250–500 kg_{Pt} GW^{-1}).[7] In that extremely challenging context, sustainable green hydrogen economy relies on efficient and systematic platinum recovery to meet the growing demand and avoid cost explosion.

Nowadays, the main part of the end-of-life platinum recycling volume is obtained from spent automotive exhaust catalysts (SAC), old jewelry and electronic wastes. In the recycling process, concentration of the platinum is estimated to 2000 g ton^{-1} compared to only 10 g ton^{-1} when using primary raw source from mining.[8] Moreover, recycling step minimizes waste production, reduces drastically environmental pollution and energy consumption down to 3.4 $\cdot 10^3$ MJ kg^{-1} compared to 2.5 10^5 MJ kg^{-1} by using primary raw material source.[9]

State-of-the-art of Pt recovery from spent automotive exhaust catalyst (SAC) at industrial scale relies on pyrometallurgy, hydrometallurgy and biohydrometallurgy processes that deliver quite high PGMs recovery yields up to 95% but face some technical issues.[10] Pyrometallurgical processes[11] require special equipment which are highly energy-intensive and generate large quantities of slag and environmental pollutants (SO_2, NO_x, CO, and dioxins).[12] Hydrometallurgy process uses highly oxidant reagents e.g., aqua regia, which is potential risk of releasing considerable amounts of NOx gases and even in aqueous solution media produces corrosive chlorine gases at higher concentrations.[13] Hydrometallurgical method is advantageous over pyrometallurgical recycling by means of operation at significantly lower temperatures, possibility for co-metal extraction, ability to be used at both small and large scale and better process control.[14,15] In some cases, a combination of both methods is employed to complete a recycling process. However, Pt recovery from MEAs containing fluorinated polymer membrane and binder materials by combining pyro and hydrometallurgical process is problematic. Thus, incineration of fluoropolymers instantly produces a risk of an extremely harmful hydrogen fluoride[16] while highly concentrated acids and oxidants such as HCl, HNO_3, and H_2O_2 readily react with fluorinated compounds and can lead to formation of high toxic vapors.[17]

Among more sustainable and mild Pt recycling methods such as electrochemical dissolution,[18,19] bioleaching,[20] transient dissolution,[21] acid and alcohol solvent process,[22] more especially, selective electrochemical dissolution method appears to be an attractive, selective strategy for Pt recovery from spent PEM cell components.[23] Diac et al.[24] demonstrated an electrochemical dissolution of Pt from spent auto catalyst as 50% recovery within 24 h in presence of chlorides containing electrolyte solution even at neutral pH. Myrzabekov et al.[25] reported electrochemical polarization under industrial scale using an alternating current source at 50 Hz, dissolution of platinum electrode with 10% current efficiency at current density of 1.5 kA m^2 in 7 M HCl to form a solution of chloroplatinic acid at room temperature. Sharma et al.[17] studied the influence of electrolyte (1 M HNO_3, 1 M H_2SO_4, 0.1 M $HClO_4$ and 1 M HCl) on dissolution of Pt from PEMFC catalysts under potentiodynamic condition. About 95% of Pt dissolution in 1 M HCl was found to be an efficient electrolyte and the dissolution rates as high as ∼30 μg/cycle for potential cycling between 0.4 and 1.6 V within 50 cycles. In all these works mentioned above, anodic polarization process was applied.

Marc Koper´s group explored the feasibility of cathodic corrosion of platinum wire by applying an AC voltage at −6 V in 10 M NaOH and observed detachment of Pt nanoparticles.[26] The

*Electrochemical Society Member.
[z]E-mail: jean-francois.drillet@dechema.de

anisotropic etching of metal electrode surface is due to strong interaction of electrolyte cation with highly negative surface charge of the electrode.[27] Feng et al.[28] extensively studied the concept of cathodic corrosion of pure metal or multi metal element alloy wire into nanoparticles (NPs) and subsequent deposition on carbon support for the use of PEMFC catalyst. This method resulted with the production rate of 30 mg h^{-1} of Pt non-aggregated NPs from bulk wire in the 1 M NaOH electrolyte solution containing 5 wt% poly(vinylpyrrolidone) (PVP) as a stabilizer under ultrasonication assisted cathodic corrosion protocol in AC voltage at −10 V with a duty cycle of 50%. One of the major issues during electrochemical cathodic Pt dissolution is related to H_2 evolution (>50 mV vs NHE) and Pt redeposition as side reactions. Sharma et al.[29] employed a second working electrode (WE2) in 1 M H_2SO_4 electrolyte solution under potentiodynamic polarization to reduce the rate of the redeposition process. Through continuous removal of dissolved Pt species by holding 0.1 V on WE2, the dissolution efficiency was increased by a factor of 2. Mitsushima et al.[30] performed the Pt dissolution from PEMFC electrode in 1 M H_2SO_4 at 40 °C under by using rectangular and triangular wave signals. By applying cathodic triangular wave protocol between 0.05 − 1.8 V at 0.5 V s^{-1}, dissolution rate was ten times higher than with fast scan rate at 20 V s^{-1}.

In some extent, Pt dissolution and recovery process in ionic liquid might present some environmental-friendly aspects.[31,32] A simultaneous recovery of platinum and electrodeposition was performed in 1-butyl-3-methylimidazolium chloride ([BMIm]Cl) and 1-butyl-3-methylimidazolium bis(trifluoromethane)sulfonimide ([BMIm]TFSI) containing 1 M chloride ions solution.[33] Sharma et al.[32] demonstrated a closed recycling loop of spent PEMFC electrode in a multi-step process including (i) Pt dissolution from dismantled MEA in 1 M HCl under potential cycling, (ii) addition of ammonium chloride, (iii) conversion of $(NH_4)_2PtCl_6$ complex, (iv) separation of precipitate by centrifugation, (v) reduction on carbon Vulcan support (20 wt% Pt/C) and finally (vi) fabrication of the electrode. Chen et al.[34] reported Pt leaching from spent electrode in 5 M HCl with 10% H_2O_2 resulting a recovery yield of 90%. However, electrochemical Pt recovery by selective dissolution from spent fuel cell compounds is a new research field with large improvement potential.

This work reports on optimization of electrochemical Pt recovery procedure from fresh and aged PEMFC electrodes by using a selective, environmentally friendly and relatively low energy-consuming approach based on electrochemical cathodic leaching (ECCL) and deposition (ECCD) of Pt in HCl solution by means of pulse voltammetry technique.

Experimental

Chemicals.—Hydrochloric acid (37%, Sigma-Aldrich), sulphuric acid (98%, Merck KGaA) were purchased and used without any further purification step. All experiments were performed with ultrapure water (>18.18 MΩ cm, Millipore, Ultra purelab ELGA).

Pt/C catalyst synthesis and GDE fabrication.—The 40 wt% Pt/C catalyst was synthesized by impregnation and reduction of corresponding amounts of hexachloroplatinic acid ($H_2PtCl_6.6H_2O$, 99.99%, Alfa Aesar) on C_{65} carbon (C-NERGY, TIMCAL, Bironico, Switzerland) in formaldehyde (CH_2O, >37%, Merck) at 80 °C for 1 h under reflux conditions. The reaction products were filtered and washed with de-ionized water through a 0.45 mm polycarbonate membrane (Sartorius AG). The obtained powder was dried at 80 °C in a vacuum furnace (VT6025, Thermo Scientific) at 50 mbar for 4 h. In this study, C_{65} carbon was utilized as catalyst support due to its superior corrosion stability under electrochemical conditions that can be assigned to its lower BET surface area of 62 m^2 g^{-1} compared to 250 m^2 g^{-1} for Vulcan XC-72R. The TEM images of carbon-supported catalysts and particle size details are provided in the SI (Fig. S1).

Typical GDE fabrication procedure was carried out as follows: 100 mg Pt/C catalyst, 20 wt% PTFE and 10 wt% Nafion were suspended in a 1:2 water:isopropanol solvent mixture and stirred for 30 min. The catalyst ink was sprayed onto a 36 cm^2 carbon paper (F-H23C6, Freudenberg) by an ultrasonic-assisted coating machine (Prism-450, Ultrasonic Systems Inc.). until getting catalyst loading of 0.4 mg_{Pt} cm^{-2}. The targeted loading was controlled by measuring the weight of electrode after each spraying step during the coating process using a precision balance (XP205, Mettler Toledo). Finally, as-coated GDEs were dried in an oven at 80 °C for 2 h.

Electrochemical tests.—Cyclic voltammograms (CV) of as-prepared and aged Pt/C gas diffusion electrodes (GDE) were recorded in a glass cell with 3 ml volume of N_2-saturated 0.5 M H_2SO_4 electrolyte using a potentiostat (PMC-1000, Princeton Applied Research, Ametek) between 0 and 1.4 V vs RHE at 40 mV s^{-1} and room temperature. A Pt wire acted as counter electrode (CE) while a reversible hydrogen electrode (RHE) (Hydroflex, Gaskatel GmbH) was used as reference electrode (RE). The electrochemical surface area (ECSA) of the catalyst was calculated by integrating the hydrogen adsorption region between 0.005 and 0.36 V vs NHE in the cyclic voltammogram (CV) and assuming that charge induced by a monolayer of hydrogen atoms on Pt amounts to 210 μC cm^{-2}. GDE aging was carried out by means of accelerated degradation tests (ADT) in a N_2-saturated 0.5 M H_2SO_4 electrolyte between 0.4 and 1.4 V at 1 V s^{-1} for 10,000 cycles.

Electrochemical dissolution tests were performed in a glass cell of 3 ml electrolyte with a two-electrode setup as shown in Fig. S2a, using a potentiostat (PMC-1000, Princeton Applied Research, Ametek) and pulse voltammetry (PV) technique. All Pt dissolution tests were performed without any inert gas purge of electrolyte. The respective electrode potentials were checked once by means of a 3-electrode set-up including a reversible hydrogen reference electrode (RHE) (see Figs. S2b–S2c). The leaching protocol was optimized by studying influence of concentration of HCl electrolyte (1–3 M), cell voltage (−1 to −9 V), duty cycle (5%–50%), and number of cycles (5–150) on dissolution rate of Pt. The duty cycle D of the rectangular pulse signal is defined as below,

$$D(\%) = \left(\frac{t_{ON}}{t_{ON} + t_{OFF}}\right) * 100 \quad [1]$$

where $t_{off} = 0$ V.

Pt electrodeposition was performed in similar glass cell using a three-electrode configuration comprising a Toray carbon gas diffusion layer (T-GDL, Toray TGP-H-060) as working (0.3 cm^2) and counter (0.5 cm^2) electrode, and a reversible hydrogen as reference electrode (RHE). The glass cell was filled with the 3 ml electrolyte providing from dissolution step with aged GDE. Electrochemical redeposition was carried by means of pulse voltammetry technique at −0.5 V cell potential, D = 33% (t_{on} = 0.3 s, t_{off} = 0.6 s) for 1300 cycles (ca. 20 min).

Post-test analysis of electrolyte solutions and GDEs.—After dissolution test, the electrolyte solution was analyzed by ICP-MS (iCAP Q, Thermo Scientific™) spectroscopy and UV–vis spectroscopy (PowerWave HT, BioTek) to determine the concentration of dissolved Pt. For latter technique, calibration experiment with standard Pt(IV) chloride solution in quartz cuvette vial in concentration range of 50–500 μM in 2 M HCl was conducted (see respective spectra in Fig. S3a). The amount of nominal Pt loading of 0.4 mg_{Pt} cm^{-2} in fresh GDE is equivalent to 307 μM of $[PtCl_6]^{2-}$ in 2 M HCl solution (Fig. S3b). It was denoted as "Ref." solution and compared with the ECCL test results.

Structural analysis of the Pt/C catalyst layer was performed by X-ray diffractometer (XRD) (D8 Advance, Bruker) equipped with Cu-$K\alpha_1$ radiation (λ = 0.154 nm). The surface morphology and the elemental mapping of the GDE layer was analyzed by scanning

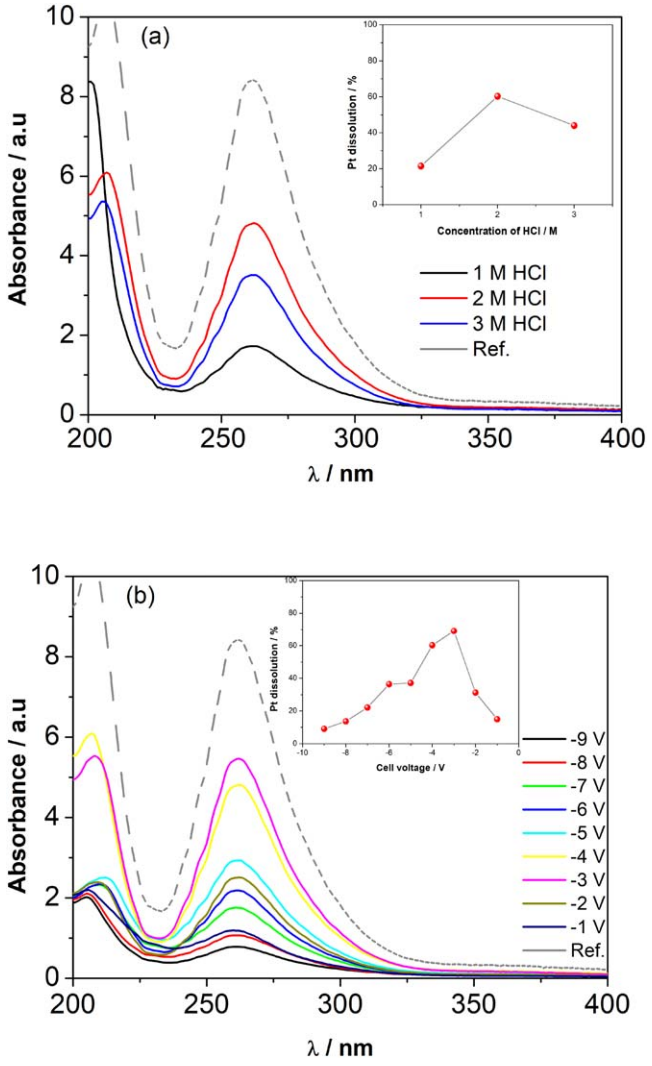

Figure 1. UV–vis spectra of Pt chloro complex in dependency of (a) HCl concentrations and (b) cell voltage in 2 M HCl. Respective Pt dissolution rates are presented in the inlet.

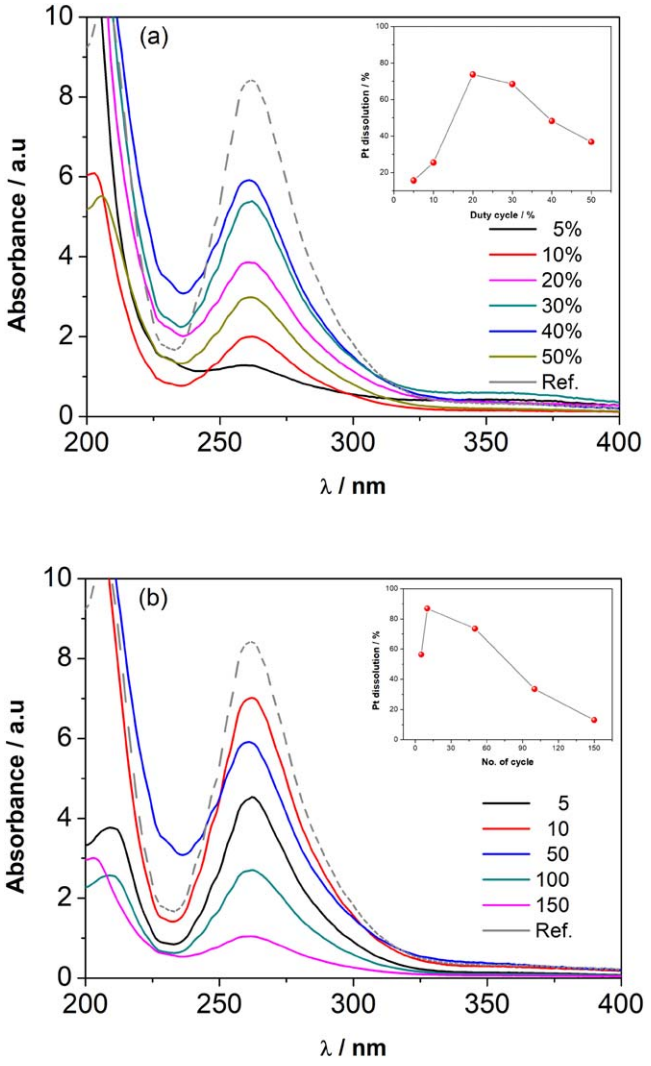

Figure 2. UV–vis spectra of Pt dissolution electrolyte by pulse voltammetry in 2 M HCl and −3 V cell voltage in dependency of (a) duty cycle D and (b) pulse number for D = 20%. Respective Pt dissolution rates are shown in the inlet.

electron microscopy (SEM) and energy dispersive X-ray spectroscopy (EDX) (FlexSEM 1000 II, Hitachi), respectively. Samples for TEM analysis were prepared by removing a small amount (∼5 mg) of the Pt/C particles from the GDE catalyst layer, which were then transferred on a Ni grid and analyzed by transmission electron microscope (TEM) (JEM-2011, JEOL at University of Saarland) at 200 kV. Amount of the Pt loading on the GDE catalyst layer was estimated by thermogravimetric analysis (TGA) (Jupiter STA 449 *F3*, Netzsch) by oxidizing all carbon content in air up to 1200 °C. The dissolution rate of catalyst in % was calculated from initial nominal (M_i) and residual (M_f) Pt loading values after test according to following equation:

$$Pt\ dissolution\ rate(\%) = \left(\frac{M_i - M_f}{M_i}\right) * 100 \qquad [2]$$

Results and Discussion

Optimization of electrochemical Pt dissolution protocol using fresh GDE.—To yield maximum Pt electrochemical dissolution from GDE layer, signal parameters such as voltage value, duty cycle, number of cycle and pulse width were investigated. The effectiveness of dissolution step was systematically evaluated by post-test analysis such as UV–vis spectroscopy of electrolyte solution, as well as CV, XRD and TGA analysis of GDE.

Effect of HCl concentration and pulse signal voltage.—The cathodic Pt dissolution process in aqueous electrolyte is unusual and faces highly competitive side reactions such as hydrogen evolution and Pt redeposition which necessitates elaborated polarization protocol. For this test, PV protocol was carried out at −4 V cell voltage, D = 30% (t_{on} = 30 s, t_{off} = 70 s) for 50 cycles. Figure 1 shows the UV–vis spectra of Pt dissolution test in different concentration of HCl electrolytes. UV–vis spectra of electrolyte after dissolution test with PV signals exhibits an absorbance peak at 260 nm which is attributed to formation of $[PtCl_6]^{2-}$ complex confirming the presence of preferential Pt(IV) ions (260 nm) to Pt(II) ions (225 nm). For comparison, a representative spectra of Pt(IV) and Pt(II) is shown in Fig. S3c. Since most commonly used Pt precursor for electrodeposition is H_2PtCl_6, the formation of chloro platinum complex in dissolution stage is an additional advantageous for transfer to one-pot (recovery & redeposition) process. The intensity of the absorption peak of Pt ions is linearly dependent on the $[PtCl_6]^{2-}$ concentration

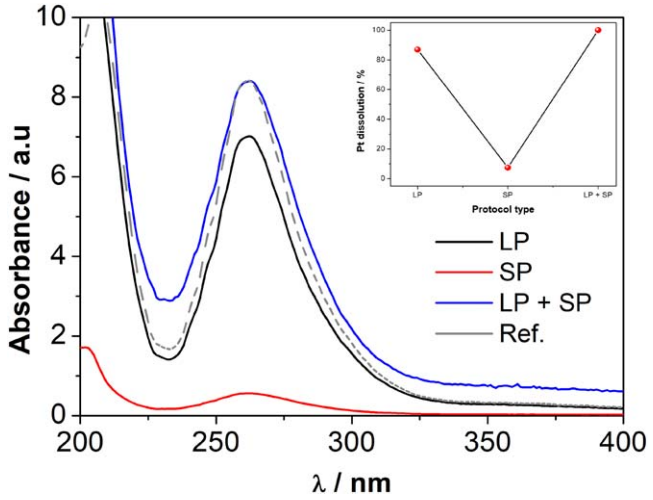

Figure 3. UV–vis spectra of electrolyte after ECCL test with different pulse protocols.

(see Fig. S3a). As shown in Fig. 1a, the UV–vis signal intensity related to Pt(IV) ($[PtCl_6]^{2-}$) species in 2 M HCl is three times higher (60%) than that in 1 M HCl solution. However, further increase in HCl concentration up to 3 M lead to a decrease in $[PtCl_6]^{2-}$ complex formation, that might be due to oxidation of chloride ions.[33] Therefore 2 M HCl concentration was selected for further experiments. Since Pt dissolution rate at −4 V cell voltage amounts only about 60% of the reference signal, next step aims to determine best performing pulse voltage value.

For the pulse voltage variation test, PV protocol was carried out in 2 M HCl electrolyte using D = 30% (t_{on} = 30 s t_{off} = 70 s) for 50 cycles. The influence of cell voltage (−1 to −9 V) on dissolved species by means of UV–Vis spectra is shown in Fig. 1b. Interestingly, absorbance signal of $[PtCl_6]^{2-}$ complex ions culminates at "only" −3 V that was calculated to 69% Pt dissolution. At more negative voltage, however, strong chlorine reduction reaction might inhibit the Pt chloro complex formation, as demonstrated by Shrestha et al.[35] At the same time, the formation of higher amount of hydrogen gas at the cathode shifts the pH value and favors the Pt re-deposition. Since at more positive cell voltage values of −2 & −1 V, dissolution yield was only 31 and 14%, respectively, the cell voltage was set to −3 V for further experiments.

Effect of duty cycle and test duration.—To further improve Pt leaching rate, influence of duty cycle D (5%–50%) was investigated in 2 M HCl using PV protocol at −3 V for 50 cycles. From Fig. 2a, it can be seen that the UV–Vis spectrum of the respective electrolyte increases until D = 20% (t_{on} = 30 s & t_{off} = 120 s) reaching a maximum dissolution yield of 73% and decreases for higher D values (Table S1). We assume that longer relaxation time t_{off} might favor a decrease in Cl^- ion concentration at the electrode/electrolyte interface and slow down Pt dissolution reaction rate. Hence, D value of 20% was chosen for further experiments.

To further optimize dissolution procedure, the influence of procedure duration on dissolution process was investigated by varying pulse number between 5 and 150 while keeping cell voltage at −3 V and using duty cycle of 20%. As can be seen in Fig. 2b, concentration of dissolved Pt(IV) ions culminates already up to 86% after 10 cycles and drops afterwards down to 73% and 13% after 50 and 150 cycles (Table S2), respectively that can be presumably attributed to excess in Pt(IV) ion concentration close to electrode/electrolyte interface and subsequent Pt redeposition process. The concentration of Pt content in electrolyte analyzed by UV–vis and ICP-MS was comparable to each other (Tables S1 & S2). Since ultimate target aimed at yielding 100% dissolution rate, additional optimization steps regarding leaching procedure were undertaken.

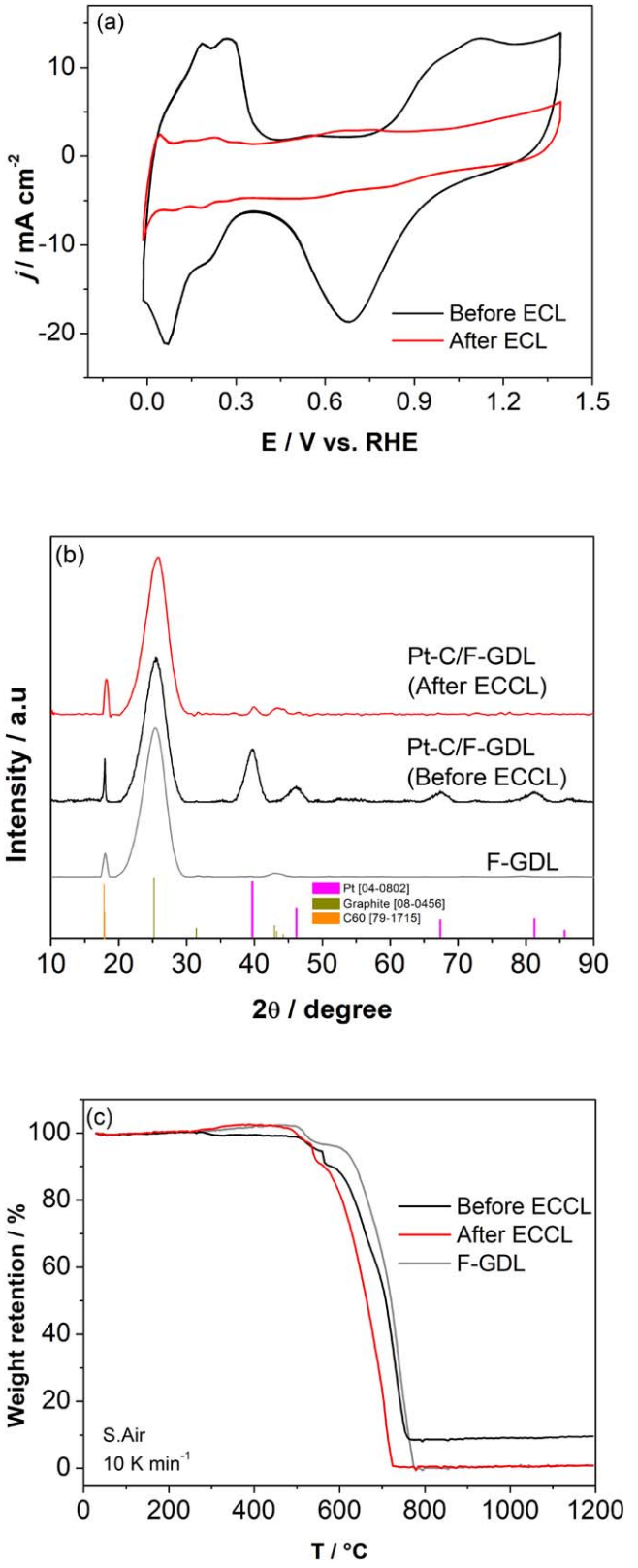

Figure 4. Evaluation of Pt dissolution from as-prepared GDE by (a) CV in N_2-saturated 0.5 M H_2SO_4 at 40 mV s^{-1}, (b) XRD pattern and (c) TGA profile of normalized weight retention of carbon and Pt.

Hence for next experiment, pulse signal profile was set to −3 V, D = 20% (t_{on} = 30 s & t_{off} = 120 s) for 10 cycles (25 min) and called "Long Pulse (LP)."

Effect of pulse profile and sequence.—The influence of pulse duration on Pt dissolution behavior from fresh GDEs was investigated by shortening LP duration by factor 10 and keeping D = 20%. The so-called "Short Pulse (SP)" consists of 100 cycles with t_{on} = 0.3 s & t_{off} = 1.2 s for a total duration of 2.5 min. The LP and SP protocols were applied either separately or combined with each other (LP + SP) as shown in Fig. S4. Figure 3 shows the UV–vis spectra of Pt-containing 2 M HCl electrolyte after the dissolution experiment with the four different pulse protocols. A notable absorbance peak intensity at 260 nm which can be attributed to $[PtCl_6]^{2-}$ complex that was detected after all experiments. The concentration of dissolved Pt(IV) was calculated to 86%, 6.5% and 99.8% for LP, SP, and LP + SP protocol, respectively. The absence of Pt re-deposition during protocol with long t_{off} (120 s) can be explained by two reasons; (i) GDE potential was about 0.8 V vs RHE which is far away from H_{upd} region and (ii) longer period for H_2 gas dilution at electrolyte/electrode interface evolved during t_{on}. It is obvious that poor efficiency of SP protocol can be attributed to short duration time of about 3 min. Interestingly, immediate succession of LP and SP protocol (LP + SP) yielded outstanding performance close to 100%. It is assumed that smaller Pt particles are completely dissolved during LP protocol, while SP signal is supposed to be more effective for the dissolution of larger, more corrosion-resistant Pt particles remaining in catalyst layer structure. For statistical purpose, five identical samples were tested under (LP + SP) polarization profile, revealing an average Pt dissolution rate of 99.8 ± 0.1%.

Balva et al.[33] reported on electrochemical anodic leaching of Pt from fresh MEA electrode at 1.3 V in a [BMIm]TFSI+[BMIm]Cl ionic liquid containing 0.1 M chloride ions at 100 °C with recovery yield of 60%. Kanamura et al.[36] recovered electrochemically in 1 M HCl at room temperature about 93% of the Pt from a MEA under square potential waves at 1.5 V for 15 s and 120 cycles (30 min). Best results in terms of recovery yield is demonstrated by Sharma et al.[37] mentioning a Pt dissolution rate of 98% from spent PEMFC electrodes under anodic cycling between 0.4 and 1.6 V at 100 mV s^{-1} in 1 M HCl excluding the risk of H_2 evolution and Pt redeposition.

To confirm excellent results from UV–vis analysis of electrolyte collected after LP + SP protocol, CV, XRD and TGA measurements of GDE were performed as well. Figure 4a shows the CV of as-prepared GDE before and after ECCL dissolution test applying LP + SP protocol. While the CV of fresh electrode exhibited all Pt characteristics regions, charge of both anodic and cathodic peaks was significantly reduced. ECSA value of GDE from cathodic H_{ads} region after dissolution test amounts to about 0.08 m^2g^{-1} compared to 51.5 m^2g^{-1} for fresh GDE, revealing a nearly complete dissolution of Pt after LP + SP procedure whereas large particles have a much lower active surface than larger ones. Surprisingly, double-capacity layer region is little affected, indicating the high corrosion stability of C_{65} carbon support.[38]

The XRD pattern of GDE before and after dissolution test displayed in Fig. 4b shows diffraction peaks at 2θ = 17.8° and 25.2° reflecting the presence of amorphous and graphitic domains in carbon from microporous layer and GDL, respectively. The carbon peaks were matches well with the standard patterns of C60 (JCPDS, 79–1715) and graphitic (JCPDS, 08–0456). While Pt diffraction peaks at 2θ = 39.5°, 46.09°, 67.55° and 81.25° matching well with

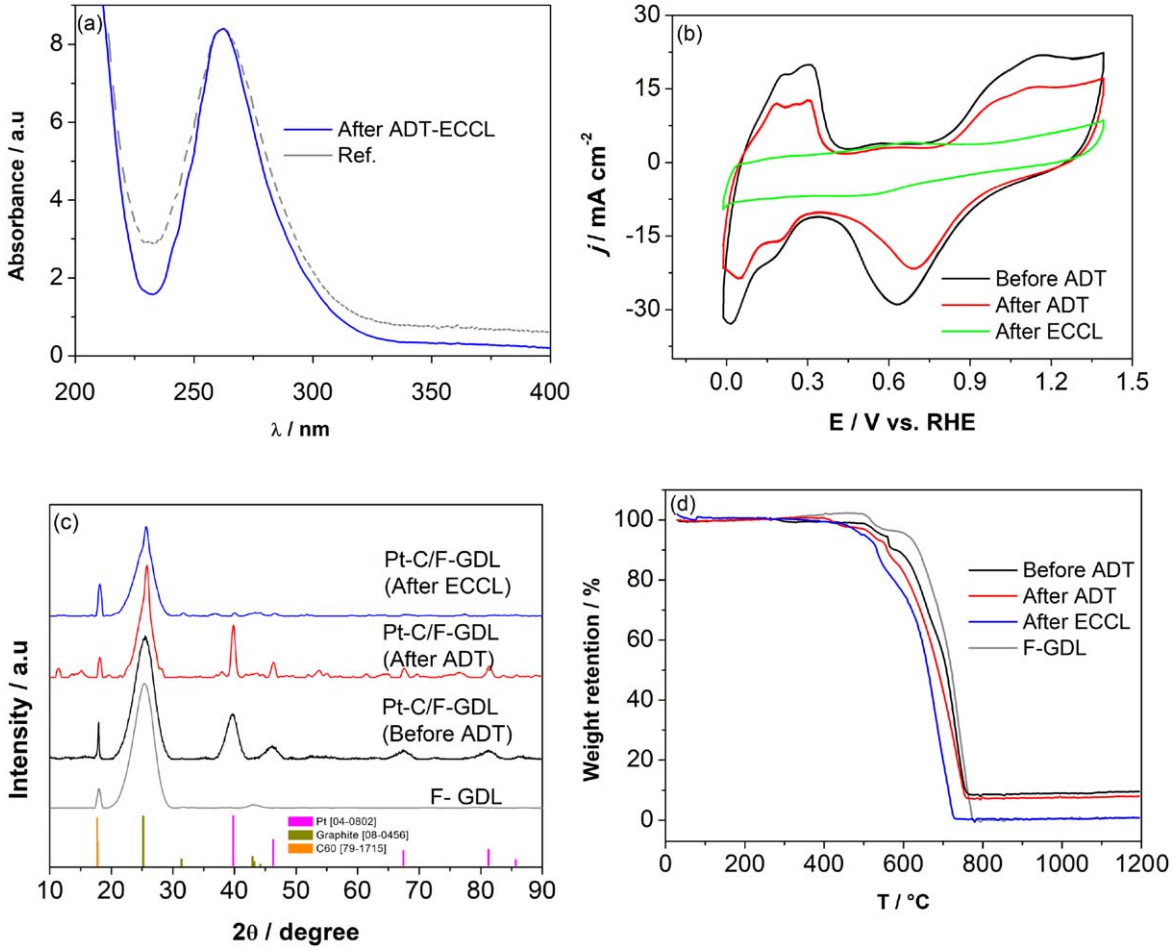

Figure 5. Evaluation of Pt dissolution rate after ECCL step using aged Pt/C GDE by means of (a) UV–vis spectra of Pt chloro complex containing electrolytes in 2 M HCl, (b) CV in N_2-saturated 0.5 M H_2SO_4 at 40 mV s^{-1}, (c) XRD pattern and (d) TGA profile of normalized weight retention of carbon and Pt.

the standard Pt pattern (JCPDS, 04–0802) are well pronounced in the pristine GDE spectrum, their intensities are strongly reduced in that of GDE after ECCL dissolution test. Since just a small peak is still visible in H_2 region of CV at 0 V, fast complete removal of Pt particles from GDE structure is assumed.

While CV and XRD techniques delivered rather a qualitative analysis of Pt dissolution rate from GDE, we expect to get more reliable information about residual Pt mass from TGA investigation since carbon is supposed to be burned at lower temperatures. The onset temperature for graphitic carbon oxidation of the pure GDL is starting at 600 °C while a total mass loss is observed at 800 °C. Figure 4c shows the TGA weight loss profile of GDE before and after electrochemical dissolution and compared with non-coated GDL as a reference. A comparable amount for sample mass of 2.3 ± 0.1 mg was kept in all experiments. Early mass gain of about 2% between 270 °C and 500 °C in the GDL is attributed to oxidation of organic compounds from the 20 wt% PTFE binder (as received) and subsequent decomposition of those compounds between 500 °C and 600 °C. However, the onset temperature for carbon oxidation and PTFE decomposition of binder from fresh GDE was shifted about 100 °C towards lower temperature compared with that of GDL due to the presence of Pt catalyst. It is well-admitted that the presence of Pt decreases the onset temperature of carbon combustion.[39] The plateau at temperatures above 800 °C reflects the residual mass of Pt (7.5% $\sim$ 0.19 mg) after complete carbon combustion that is consistent with the nominal weight of Pt loading on the GDE i.e., 40 wt% Pt/C. As expected, the TGA curve of GDE after ECCL test exhibited similar behavior to that of GDL profile that is a reliable indication for complete Pt dissolution. Furthermore, all these three investigations on GDE further validate the concentration of Pt in the electrolyte determined from UV–vis spectrum of LP + SP shown in Fig. 3.

Experiments with aged Pt/C GDE.— *Electrochemical Pt dissolution from aged GDE.*—In this work, the aging of GDE was achieved by applying an accelerated degradation test (ADT) protocol. Figure 5a shows CV of GDE before and after ADT cycles and subsequently ECCL procedure using LP + SP protocol specified in the previous section. Significant ECSA loss of about 41% and 100% was observed in GDEs with Pt/C catalysts after 10,000 ADT cycles and subsequent dissolution test, respectively. Since the current density in double-layer capacitance region is moderately affected by ADT procedure, ECSA loss is principally assigned to rather Pt degradation mechanisms such as migration, Oswald ripening, coalescence, dissolution, precipitation, and detachment than to oxidation of carbon support.[36] After both ADT and ECCL procedure, the CV shape is typical for that of pure carbon support material.

The concentration of Pt (IV) complex in dissolution bath evaluated from UV–vis spectrum was measured to about 307 μM which correlating to 100% of dissolution (see Fig. 5d). The XRD pattern of GDE after ADT and dissolution test is shown in Fig. 5b. The Pt and carbon peak positions are in good agreement with the standard Pt pattern. Interestingly, after ADT test, the width of Pt diffraction peaks is narrower indicating an increase in crystallinity and particle size during the aging process. After ECCL dissolution test, the Pt diffraction peaks were almost vanished confirming the huge removal of Pt particles from GDE structure. Figure 5c shows

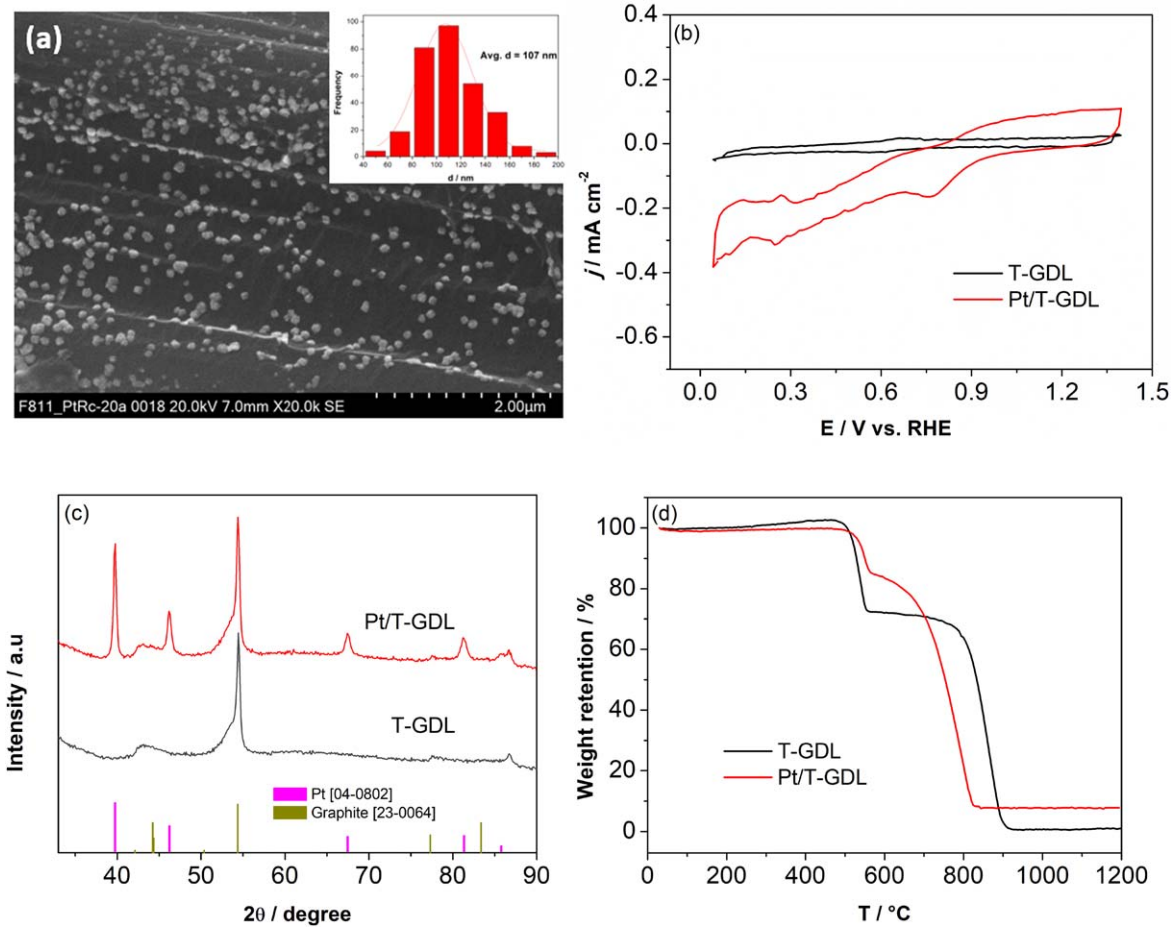

Figure 6. Characteristics of GDE by pulse deposition of Pt on T-GDL from (a) SEM images of Pt/T-GDL with corresponding Pt particle size distribution histograms, (b) CV profile in N_2-saturated 0.5 M H_2SO_4 at 40 mV s^{-1}, (c) XRD pattern and (d) TGA profile of GDL and electrodeposited Pt/GDL catalyst. The characteristics of blank Toray GDL is included for comparison in (b)–(d).

the TGA weight loss profile of GDE before and after aging electrochemical dissolution. The weight loss profile was similar to those shown in Fig. 4c, notable difference in Pt loading i.e., weight loss of 15% was estimated from the aged GDE. Pt dissolution was estimated between aged GDE and after ECCL test profile after 800 °C similar to that of the GDL profile that indicates the complete Pt dissolution.

One-pot electrochemical Pt redeposition on GDL.— Electrochemical cathodic deposition (ECCD) was performed at −0.5 V, D = 33%, and 1,300 cycles for ca. 20 min using 2 M HCl-based ECCL dissolution bath. Figure 6a shows the SEM image of well-dispersed electrodeposited Pt on carbon fiber of T-GDL at −0.5 V with the corresponding histogram revealing a very large mean particle size of about 107 nm. Figure 6b shows the CV of electrodeposited Pt on T-GDL for 20 min as well as that of the non-coated GDL for comparison.

The very low ECSA value of 0.5 m^2g^{-1} was calculated from H_{ads} region and it can be assigned to deposition of very large Pt particle size. Optimization of electroplating protocol for obtaining Pt particles in the range of 3–10 nm is very challenging and out of the scope of this work. In this study, Pt redeposition experiment should be considered as a proof of concept for one-pot electrochemical recovery of Pt in diluted HCl solution. The quality of Pt deposition after ECCD test was confirmed by XRD as shown in Fig. 6c. The Pt and carbon peak positions are in good agreement with the standard Pt pattern. After ECCD, the Pt diffraction peaks were narrow that indicates an increase in crystallinity and deposition of larger size particles. The amount of electrodeposited Pt loaded on GDL from one-pot experiment was evaluated by TGA experiment in oxidative atmosphere up to 1200 °C where TGA profile of uncoated GDL serves as reference (see Fig. 6d). The first weight loss of about 30% at 500 °C is associated with the evaporation of fluorine content from the PTFE treated Toray paper of GDL. Interestingly, the presence of Pt reduces the weight loss to about 15% in that temperature window and slightly favors the carbon combustion at higher temperature that is completely oxidized in 800 °C–900 °C region. Therefore, the weight retention in the plateau region after 900 °C amounting 7.9% (2.4 mg) is assigned to Pt mass only. Finally, Pt recovery efficiency of 87.5% was determined by calculating the ratio of Pt loading of 0.35 mg_{Pt} cm^{-2} after electrochemical deposition and that after ECCL step of aged GDE from TGA profile. Figure S5 shows the comparison of UV–vis spectra electrolyte solution before and after Pt deposition. The differences in the absorption peak intensity were about 87% which directly correlates to the amount of Pt deposit and well agreed with TGA results. An improved recovery efficiency and smaller Pt particle size can be achieved by optimizing the electrodeposition protocol parameters.

Conclusions

In this work, the feasibility of electrochemical cathodic leaching (ECCL) and deposition of platinum from gas diffusion electrodes (GDEs) in the same solution was successfully demonstrated by using pulse voltammetry (PV) in one pot method for the first time. The optimization of ECCL protocol was performed with as-prepared GDEs by optimizing HCl electrolyte concentration, cell voltage, duty cycle, leaching duration and pulse sequence. The best combination in terms of leaching efficiency was obtained by applying successively a long and short pulse sequence between 0 and −3 V (cathode potential −0.55 V vs RHE) with a duty cycle D of 20% in 2 M HCl for 30 min. The method was very successful in achieving Pt leaching rate up to 99.8 ± 0.1% from both fresh and aged GDEs. The preferential formation of $[PtCl_6]^{2-}$complexes in the dissolution bath was confirmed by UV–vis analysis and ICP-MS. The calculated Pt amounts from dissolution bath (UV–vis) and GDE (ECSA) are in very good agreement. This work describes a kind of guideline for designing of a successful electrochemical Pt leaching process using pulse voltammetry technique. For sure, this protocol should be adapted to cell design, electrolyte volume as well as catalyst nature, loading and particle size. For higher electrode surface and consequently electrolyte volumes, H_2 evolution side reaction should be considered. Moreover, $[PtCl_6]^{2-}$complex-containing dissolution bath can be immediately or after purification step re-used for one-pot Pt recovery step paving the way for more efficient and affordable circular economy, more especially when recycling GDE with very low PGM material loading.

Acknowledgments

The authors are very grateful for financial support by the “Hessen Agentur GmbH” within the framework of e-mobility program in Hesse (“Pt2Go2Pt” Grant no. 847/20–07). We also thank Dr. Christian Gebauer and Dr. Bernhard Bauer-Siebenlist from Heraeus Precious Metals GmbH & Co. KG. for fruitful discussion during the project meetings.

ORCID

Mariappan Sakthivel https://orcid.org/0000-0002-9514-7851
Jean-Francois Drillet https://orcid.org/0000-0002-4838-5195

References

1. Hydrogen Council Report, (2020), https://hydrogencouncil.com/en/path-to-hydrogen-competitiveness-a-cost-perspective/ (last accessed on10th July 2025).
2. J. Matthey, (2024), https://matthey.com/products-and-markets/pgms-and-circularity/pgm-markets/pgm-market-reports (last accessed on10th July 2025).
3. European Commission, (2020), https://op.europa.eu/en/publication-detail/-/publication/c0d5292a-ee54-11ea-991b-01aa75ed71a1/language-en (last accessed on10th July 2025).
4. Y. Wang, Y. Pang, H. Xu, A. Martinez, and K. S. Chen, *Energy Environ. Sci.*, **15**, 2288 (2022).
5. www.energy.gov/eere/fuelcells/doe-technical-targets-fuel-cell-systems-and-stacks-transportation-applications (last accessed 06th June 2025).
6. B. G. Pollet, S. S. Kocha, and I. Staffell, *Curr. Opin. Electroche.*, **16**, 90 (2019).
7. M. Bernt, A. Hartig-Weiß, M. F. Tovini, H. A. El-Sayed, C. Schramm, J. Schröter, C. Gebauer, and H. A. Gasteiger, *Chem. Ing. Tech.*, **92**, 31 (2020).
8. M. Gislev and M. Grohol, (2018), https://op.europa.eu/en/publication-detail/-/publication/d1be1b43-e18f-11e8-b690-01aa75ed71a1.
9. B. J. Glaister and G. M. Mudd, *Miner. Eng.*, **23**, 438 (2010).
10. S. Karim and Y.-P. Ting, *Resour. Conserv. Recycl.*, **170**, 105588 (2021).
11. G. Kolliopoulos, E. Balomenos, I. Giannopoulou, I. Yakoumis, and D. Panias, *Open Access Library Journal*, 1 e736 (2014).
12. Z. Peng, Z. Li, X. Lin, H. Tang, L. Ye, M. Rao, Y. Zhang, G. Li, and T. Jiang, *JOM*, **69**, 1553 (2017).
13. M. K. Jha, J.-C. Lee, M.-S. Kim, J. Jeong, B.-S. Kim, and V. Kumar, *Hydrometallurgy*, **133**, 23 (2013).
14. C. Saguru, S. Ndlovu, and D. Moropeng, *Hydrometallurgy*, **182**, 44 (2018).
15. B. Xu, Y. Chen, Y. Zhou, B. Zhang, G. Liu, Q. Li, Y. Yang, and T. Jiang, *Metals*, **12**, 533 (2022).
16. R. Wittstock, A. Pehlken, and M. Wark, *Recycling*, **1**, 343 (2016).
17. R. Sharma, K. R. Nielsen, P. B. Lund, S. B. Simonsen, L. Grahl-Madsen, and S. M. Andersen, *Chem. Electro. Chem.*, **6**, 4471 (2019).
18. W. Jin and Y. Zhang, *ACS Sustainable Chem. Eng.*, **8**, 4693 (2020).
19. P. Halli, J. J. Heikkinen, H. Elomaa, B. P. Wilson, V. Jokinen, K. Yliniemi, S. Franssila, and M. Lundström, *ACS Sustainable Chem. Eng.*, **6**, 14631 (2018).
20. A. Pathak, H. Al-Sheeha, R. Navvamani, R. Kothari, M. Marafi, and M. S. Rana, *Rev. Environ. Sci. Biotechnol.*, **21**, 1035 (2022).
21. N. Hodnik, C. Baldizzone, G. Polymeros, S. Geiger, J. P. Grote, S. Cherevko, A. Mingers, A. Zeradjanin, and K. J. J. Mayrhofer, *Nat. Commun.*, **7**, 13164 (2016).
22. J. Moon, S. Nishihama, and K. Yoshizuka, *Solvent Extr. Ion Exc.*, **36**, 470 (2018).
23. R. Sharma, S. B. Simonsen, P. Morgen, and S. M. Andersen, *Electrochim. Acta*, **321**, 134662 (2019).
24. C. Diac, F. I. Maxim, R. Tirca, A. Ciocanea, V. Filip, E. Vasile, and S. N. Stamatin, *Metals*, **10**, 822 (2020).
25. B. E. Myrzabekov, A. B. Bayeshov, A. B. Makhanbetov, B. Mishra, and O. S. Baigenzhenov, *Metall. Mater. Trans. B*, **49**, 23 (2018).
26. A. I. Yanson, P. V. Antonov, P. Rodriguez, and M. T. M. Koper, *Electrochim. Acta*, **112**, 913 (2013).
27. A. I. Yanson, P. Rodriguez, N. Garcia-araez, R. V. Mom, F. D. Tichelaar, and M. T. M. Koper, *Angew. Chem. Int. Ed.*, **50**, 6346 (2011).
28. J. Feng, D. Chen, A. S. Sediq, S. Romeijn, F. D. Tichelaar, W. Jiskoot, J. Yang, and M. T. M. Koper, *ACS Appl. Mater. Interfaces*, **10**, 9532 (2018).
29. R. Sharma, S. Gyergyek, and S. M. Andersen, *Chem. Sus. Chem.*, **11**, 3742 (2018).
30. S. Mitsushima, S. Kawahara, K. Ota, and N. Kamiya, *J. Electrochem. Soc.*, **154**, B153 (2007).
31. M. Matsumiya, Y. Song, Y. Tsuchida, H. Ota, and K. Tsunashima, *Sep. Purif. Technol.*, **214**, 162 (2019).

32. M. Chen, S. Li, C. Jin, M. Shao, and Z. Huang, *Sep. Purif. Technol.*, **259**, 118204 (2021).
33. M. Balva, S. Legeai, N. Leclerc, E. Billy, and E. Meux, *Chem. Sus. Chem*, **10**, 2922 (2017).
34. W. S. Chen, W. S. Liu, and W. C. Chen, *Metals*, **13**, 1006 (2023).
35. B. R. Shrestha, E. Tada, and A. Nishikata, *Electrochi. Acta*, **143**, 161 (2014).
36. S. Kanamura and M. Yagyu, *Mater. Trans.*, **57**, 1972 (2016).
37. N. Bogolowski, O. Ngaleu, M. Sakthivel, and J.-F. Drillet, *Carbon*, **119**, 511 (2017).
38. M. Sakthivel and J. F. Drillet, *Appl. Catal., B*, **231**, 62 (2018).
39. R. Sharma, S. J. Andreasen, J. Chamier, and S. M. Andersen, *J. Electrochem. Soc.*, **166**, F963 (2019).